A Kinetic Assessment of the Sequence of Electron Transfer from F_X to F_A and Further to F_B in Photosystem I: The Value of the Equilibrium Constant between F_X and F_A

Vladimir P. Shinkarev,* Ilya R. Vassiliev,† and John H. Golbeck†

*Department of Plant Biology, University of Illinois, Urbana, Illinois 61801, and †Department of Biochemistry and Molecular Biology, Pennsylvania State University, University Park, Pennsylvania 16802 USA

ABSTRACT The x-ray structure analysis of photosystem I (PS I) crystals at 4-Å resolution (Schubert et al., 1997, *J. Mol. Biol.* 272:741–769) has revealed the distances between the three iron-sulfur clusters, labeled F_X, F_1, and F_2, which function on the acceptor side of PS I. There is a general consensus concerning the assignment of the F_X cluster, which is bound to the PsaA and PsaB polypeptides that constitute the PS I core heterodimer. However, the correspondence between the acceptors labeled F_1 and F_2 on the electron density map and the F_A and F_B clusters defined by electron paramagnetic resonance (EPR) spectroscopy remains controversial. Two recent studies (Diaz-Quintana et al., 1998, *Biochemistry.* 37:3429–3439; Vassiliev et al., 1998, *Biophys. J.* 74:2029–2035) provided evidence that F_A is the cluster proximal to F_X, and F_B is the cluster that donates electrons to ferredoxin. In this work, we provide a kinetic argument to support this assignment by estimating the rates of electron transfer between the iron-sulfur clusters F_X, F_A, and F_B. The experimentally determined kinetics of $P700^+$ dark relaxation in PS I complexes (both F_A and F_B are present), $HgCl_2$-treated PS I complexes (devoid of F_B), and P700-F_X cores (devoid of both F_A and F_B) from *Synechococcus* sp. PCC 6301 are compared with the expected dependencies on the rate of electron transfer, based on the x-ray distances between the cofactors. The analysis, which takes into consideration the asymmetrical position of iron-sulfur clusters F_1 and F_2 relative to F_X, supports the $F_X \rightarrow F_A \rightarrow F_B \rightarrow Fd$ sequence of electron transfer on the acceptor side of PS I. Based on this sequence of electron transfer and on the observed kinetics of $P700^+$ reduction and F_X^- oxidation, we estimate the equilibrium constant of electron transfer between F_X and F_A at room temperature to be ~47. The value of this equilibrium constant is discussed in the context of the midpoint potentials of F_X and F_A, as determined by low-temperature EPR spectroscopy.

INTRODUCTION

Photosystem I (PS I) of oxygenic photosynthesis is a membrane-bound protein-cofactor complex that functions as a light-dependent plastocyanin (or cytochrome c_6):ferredoxin (or flavodoxin) oxidoreductase. Light-induced electron transfer takes place in a series of reactions between neighboring electron carriers that are embedded in this protein complex. The electron carriers include a dimeric chlorophyll (Chl), which functions as the primary electron donor (P700); a monomeric chlorophyll, which functions as the primary electron acceptor (A_0); an intermediate quinone electron carrier (A_1); and three [4Fe-4S] clusters (F_X, F_A, and F_B), which operate as the terminal electron acceptors. The cofactors P700, A_0, A_1, and F_X are bound to the two main polypeptides, PsaA and PsaB, and the terminal electron acceptors F_A and F_B are bound to the small PsaC subunit (reviewed in Golbeck, 1995; Brettel, 1997; Fromme, 1999; Manna and Chitnis, 1999).

X-ray structure analysis of PS I crystals at 4 Å resolution (Schubert et al., 1997; Klukas et al., 1999) has revealed the distances between the three iron-sulfur clusters F_X, F_1, and F_2, which function on the acceptor side of PS I. There is a general consensus on the assignment of the F_X cluster that is bound to the PsaA and PsaB polypeptides that constitute the PS I core heterodimer. However, the correspondence of the F_1 and F_2 clusters defined by the x-ray data to the F_A and F_B clusters defined by their electron paramagnetic resonance (EPR) spectra and cysteine ligands on PsaC remains controversial (reviewed in Brettel, 1997; Kamlowski et al., 1997; Vassiliev et al., 1998). In particular, the definite assignment of F_A and F_B to electron density depends on nonsymmetry elements in the polypeptide backbone of PsaC, which are difficult to resolve on the 4-Å map.

The following are the main kinetically based findings concerning the function of the iron-sulfur clusters F_A and F_B in PS I:

1. Removal of PsaC by treatment with chaotropic agents leads to the loss of $NADP^+$ photoreduction. Rebinding of PsaC to isolated P700-F_X core restores $NADP^+$ photoreduction (Hanley et al., 1992).

2. Treatment of chloroplasts and PS I complexes with $HgCl_2$, which leads to selective inactivation of F_B, inhibits $NADP^+$ (Fujii et al., 1990), ferredoxin, and flavodoxin photoreduction (Jung et al., 1995; Diaz-Quintana et al., 1998; Vassiliev et al., 1998).

3. Cluster F_B is the main site of electron donation to methyl viologen (Fujii et al., 1990).

Received for publication 6 July 1999 and in final form 19 October 1999.

Address reprint requests to Dr. John H. Golbeck, Department of Biochemistry and Molecular Biology, Pennsylvania State University, S-310 Frear Laboratory, University Park, PA 16802-4500. Tel.: 1-814-864-1163; Fax: 814-863-7405; E-mail: jhg5@psu.edu.

Dr. Vassiliev is on leave from the Department of Biophysics, Faculty of Biology, M. V. Lomonosov Moscow State University, Moscow 119899, Russia.

0006-3495/00/01/363/10 $2.00

4. Cluster F_A can still be photochemically reduced despite the absence of F_B (Golbeck and Warden, 1982; Fujii et al., 1990) and can donate electrons to methyl viologen added in high concentrations (Fujii et al., 1990; Vassiliev et al., 1998).

5. Both the amplitude and the decay rate of A_{430} of $HgCl_2$-treated particles are very similar to that of untreated particles, with lifetimes in both cases of ~40–45 ms (He and Malkin, 1994);

6. The amplitude of the photovoltage change is lower in $HgCl_2$-treated PS I complexes than in the presence of F_B (Mamedov et al., 1998; Diaz-Quintana et al., 1998).

7. In spinach, inactivation of cluster F_B by $HgCl_2$ inhibits electron transfer to the water-soluble electron acceptor ferredoxin. However, the restoration of F_B in PS I does not lead to the restoration of ferredoxin and $NADP^+$ reduction (He and Malkin, 1994).

8. In cyanobacteria, reconstitution of iron-sulfur cluster F_B with β-mercaptoethanol, inorganic iron, and sulfide results in restoration of $NADP^+$ (Jung et al., 1995), ferredoxin, and flavodoxin (Jung et al., 1995; Diaz-Quintana et al., 1998; Vassiliev et al., 1998) photoreduction.

These findings imply that $F_1 \equiv F_A$ and $F_2 \equiv F_B$. A similar conclusion regarding the positions of F_A and F_B relative to F_X has been reached using site-directed mutants with substitutions of the ligands to F_A and F_B (Golbeck, 1999) or charged amino acids surrounding F_A and F_B (Fischer et al., 1997, 1999).

Although arguments have been put forward which state that F_A is distal to F_X (values of redox potentials of F_A and F_B, the absence of photoreduction of F_A in chloroplasts with F_B modified by diazonium benzene sulfonate; Malkin, 1984, and others; see Brettel, 1997, and Scheller et al., 1997, for discussions), the kinetic data are largely consistent with the assignment of F_B as the terminal electron acceptor (particularly the requirement of the presence of F_B for $NADP^+$ photoreduction and the accessibility of F_B to exogenous (O_2, MV) and endogenous (ferredoxin, flavodoxin) acceptors).

A general consideration of the effect of distance on the rate of electron transfer has been applied by Brettel (1997) to the analysis of structure-function relationships in PS I and, in particular, to electron transfer between the iron-sulfur clusters. Here we further elaborate on these considerations to assign the F_1 and F_2 iron-sulfur clusters in PS I to F_A and F_B. It is shown that the kinetics of $P700^+$ dark relaxation in Hg-treated (only F_A is present) PS I complexes from *Synechococcus* sp. are consistent with the identification $F_1 = F_A$. Thus the analysis of flash-induced kinetics of $P700^+$ based on rate versus distance relationships strongly supports the following sequence of electron transfer on the acceptor side of PS I: $F_X \rightarrow F_A \rightarrow F_B \rightarrow Fd$.

MATERIALS AND METHODS

Isolation of PS I complexes

PS I complexes from *Synechococcus* sp. PCC 6301 (TX-PS I) were isolated using Triton X-100 and sucrose gradient ultracentrifugation (Golbeck, 1995). Isolated PS I preparations were resuspended in 50 mM Tris buffer, pH 8.3, with 15% glycerol, frozen as small aliquots in liquid nitrogen and stored at −95°C before use. The preparation of F_B-less, Hg-treated TX-PS I complexes and the reinsertion of the F_B iron-sulfur cluster were performed as described previously (Jung et al., 1995) by adaptation of the original protocol developed for higher plants (Sakurai et al., 1991) to cyanobacteria. To obtain kinetic confirmation for the removal of a single iron-sulfur cluster, we employed ΔA_{832} measurements and a multiple flash excitation protocol developed by Sauer and co-workers (1978). An independent estimation of F_A and F_B content is provided by low-temperature EPR spectroscopy. Both approaches showed that treatment of the cyanobacterial PS I complexes with $HgCl_2$ resulted in 90% destruction of the F_B iron-sulfur cluster and in the retention of 80% of the F_A iron-sulfur cluster (data not shown). Damage to the F_X cluster during the PS I complex isolation and subsequent $HgCl_2$ treatment can be best assessed by estimating the contribution of the F_X back-reaction to $P700^+$ reduction in the presence of methyl viologen. As follows from the kinetics measured in previous work (Vassiliev et al., 1998) for the same material as used in the present work, less than 8% of F_A and F_B is missing in the control, and less than 10% of F_X is damaged in the Hg-treated sample.

Time-resolved absorbance spectroscopy

Samples for optical experiments were suspended anaerobically in 25 mM Tris buffer (pH 8.3) in quartz cuvettes with airtight stoppers. Triton X-100 was added to a final concentration of 0.04% to reduce light scattering. 2,6-Dichlorophenol-indophenol (DCPIP), sodium ascorbate, and methyl viologen (all from Sigma, St. Louis, MO) were added where indicated. The solutions were prepared in an anaerobic chamber using oxygen-free distilled water, with air replaced in a Thunberg tube by high-purity nitrogen.

The kinetics of the absorbance changes at 832 nm (ΔA_{832}) and at 811 nm (ΔA_{811}) were measured in a 10 mm × 4 mm cuvette placed in a laboratory-built spectrophotometer described previously (Vassiliev et al., 1998). The kinetics of the absorbance changes in the visible region were measured with a custom-built single-beam spectrophotometer. A collimated beam derived from a 400-W tungsten bulb was passed through a 5-cm water filter and a Jarrel Ash monochromator (slits set to provide 5-nm bandwidths, FWHM), and the collimated beam was passed through a 10 mm × 10 mm cuvette containing the sample. An identical monochromator was placed between the sample and a negatively biased photodetector (PIN-10D; United Detector Technology, Hawthorne, CA). The photocurrent was converted to voltage with a 10-kΩ resistor and amplified 500-fold with an EG&G model 113A amplifier (bandwidth 100 kHz). The kinetics were averaged 32 times and digitized with a Nicolet 4094A oscilloscope interfaced via a NB-GPIB/TNT board (National Instruments, Austin, TX) to a Macintosh 7100/80 computer. To reduce exposure of the sample to actinic light, a Uniblitz VS25 shutter (Vincent Associates, Rochester, NY) was placed between the first monochromator and the sample. The shutter was opened 5 ms in advance of the excitation flash for a total period of 100 ms. In both NIR and visible kinetic measurements, single turnover flashes were provided by a frequency-doubled (λ, 532 nm), Q-switched (FWHM, 10 ns) Nd-YAG laser model DCR-11 (Spectra-Physics, Mountain View, CA) at a flash energy of 10 mJ. The intervals between the flashes were 9 s for the P700-F_X core and 50 s in all other preparations. The multiexponential fits of ΔA_{832} kinetics were performed by the Marquardt algorithm in Igor Pro, version 3.14 (Wavemetrics, Lake Oswego, OR).

RESULTS

Kinetics of $P700^+$ dark relaxation in control (F_A and F_B present) PS I complexes in the presence of a slow donor (DCPIP)

Fig. 1 shows typical kinetic traces of the flash-induced absorbance change at 832 nm in an integral (F_A/F_B) TX-PS I

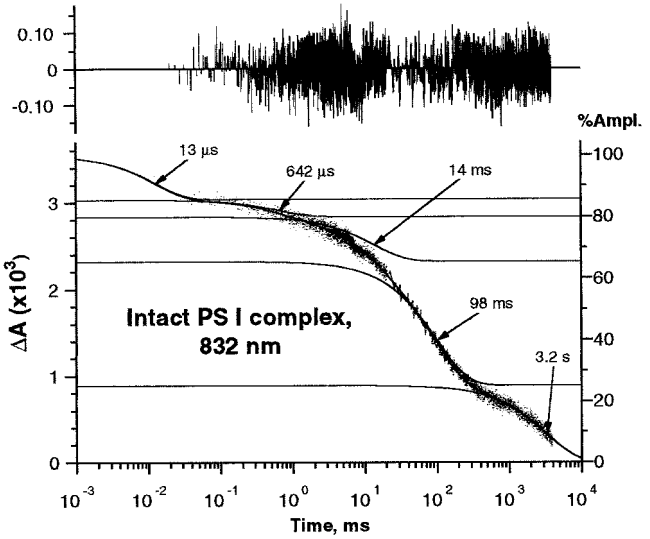

FIGURE 1 Kinetics of absorbance changes at 832 nm in integral (F_AF_B) TX-PS I complexes from *Synechococcus* sp. PCC6301. Reaction medium (anaerobic): 25 mM Tris buffer (pH 8.3), 0.04% Triton X-100, 4 μM DCPIP, and 10 mM Na ascorbate. Chl *a* concentration, 50 μg/ml. Each component of the multiexponential fit is plotted with a vertical offset relative to the next component (with a longer lifetime) or the baseline; the offset is equal to the amplitude of the latter component.

complex from *Synechococcus* sp. PCC 6301 in the presence of DCPIP and ascorbate. The ΔA_{832} kinetics, which reflects the $P700^+$ dark relaxation, is presented on a logarithmic time scale so that the charge recombination from A_1^- through F_A^- can be visualized. The multiexponential fit of these kinetics shows at least five different components with characteristic lifetimes of ~13 μs, 642 μs, 14 ms, 98 ms, and 3.2 s and amplitudes of ~14, 5.6, 14.5, 40.3, and 25.1%, respectively.

The different components of $P700^+$ dark relaxation can be identified using preparations missing some or all of the iron-sulfur clusters. $P700^+$ reduction in P700-F_X cores (without F_A/F_B) is dominated by kinetic components with lifetimes of ~0.2 ms and 2 ms, which represent, either directly or indirectly (through A_1), the back-reaction from F_X^- (Vassiliev et al., 1997; see also Figs. 3 and 4 below). Similarly, $P700^+$ reduction in P700-A_1 cores (without F_X and F_A/F_B) is dominated by kinetic components with lifetimes of ~10 and 70 μs, which represents, either directly or indirectly (through A_0), the back-reaction from A_1^- (Brettel and Golbeck, 1995). In addition, the decay of the triplet state of chlorophyll (Brettel and Golbeck, 1995; Vassiliev et al., 1997) contributes to the tens-of-microseconds kinetic phase, but this can be differentiated from the A_1 back-reaction by a flash saturation study and a wavelength dependence in the near-IR. Note that the above kinetic assignments only apply to reaction centers with missing iron-sulfur clusters; they do not pertain to reaction clusters with prereduced iron-sulfur clusters, where electrostatic interactions between iron-sulfur clusters may affect the kinetics and/or midpoint potentials of the acceptors (see Brettel, 1997). Because freshly isolated membranes show flash-induced kinetics with almost exclusively the millisecond and second components present (Vassiliev et al., 1997), the faster phases in TX-PS I complexes most likely result from differential damage to the iron-sulfur clusters in a minority of detergent-isolated PS I complexes. The slower millisecond components (~10 and 200 ms) are due to charge recombination between $[F_A/F_B]^-$ and $P700^+$. The slowest (seconds) component was assigned to the reduction of $P700^+$ by DCPIP (for discussion see Vassiliev et al., 1997).

Kinetics of P700 dark relaxation in $HgCl_2$-treated (F_B-less) PS I complexes in the presence of a slow electron donor for $P700^+$

Fig. 2 shows the kinetic trace of the absorbance change at 832 nm in a TX-PS I complex treated with $HgCl_2$ to remove the F_B iron-sulfur cluster. The multiexponential fit of these kinetics shows components with characteristic lifetimes of ~12 μs, 208 μs, 3 ms, 18 ms, and 112 ms and amplitudes of ~19.3, 8.3, 7.8, 44.2, and 18.2%, respectively. The slowest component is approximated by a baseline that contributes 2.2% to the overall amplitude. Thus the main effect of the $HgCl_2$ treatment is an increase of the contribution from the millisecond components of the $P700^+$ dark relaxation at the expense of the slow (seconds) component due to $P700^+$ reduction by DCPIP. The fraction of these millisecond components is increased from ~55% in control TX-PS I complexes to ~70% in a TX-PS I complex treated with $HgCl_2$.

The result of the effect of $HgCl_2$ on the kinetics of $P700^+$ dark relaxation agrees well with similar results obtained for

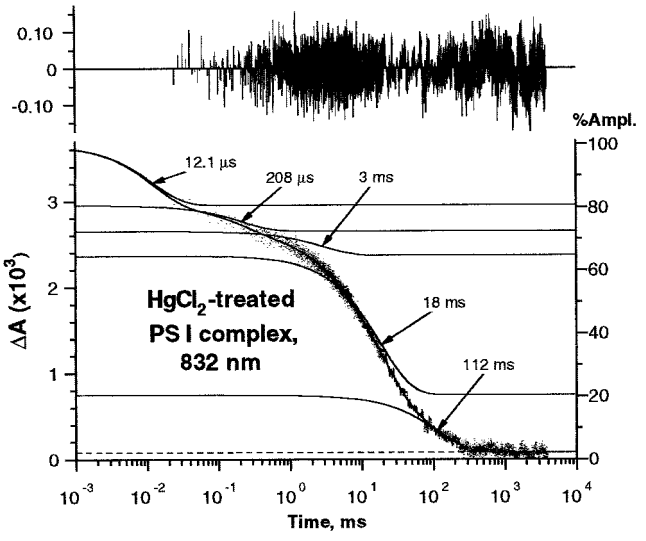

FIGURE 2 Kinetics of absorbance change at 832 nm in $HgCl_2$-treated PS I complexes from *Synechococcus* sp. PCC6301. The reaction medium is as in Fig. 1.

spinach (He and Malkin, 1994) and *Synechocystis* sp. PCC 6803 (Diaz-Quintana et al., 1998). In previous experiments on $HgCl_2$-treated PS I complexes from *Synechococcus* sp. PCC 6301 (Vassiliev et al., 1997), we reported a significant amplitude of the submillisecond component due to electron transfer from F_X^- to $P700^+$ in RCs with a damaged F_A cluster. This component is practically absent (<10%) in preparations used in the present (this work) and previous (Vassiliev et al., 1998) studies, attesting to the low amount of damage to F_A in these preparations.

Kinetics of dark relaxation in PS I core (F_A/F_B-less) complexes

To monitor the kinetics of the back-reaction between F_X^- and $P700^+$ we studied core PS I complexes where both F_A and F_B are absent. Fig. 3 shows the multiexponential fit of the kinetics of $P700^+$ dark relaxation in P700-F_X core complexes measured at 811 nm. The observed absorbance change has components with characteristic times of ~9 μs, 103 μs, 576 μs, and 3.6 ms and amplitudes ~9.2, 7.6, 71.2, and 7.2%, respectively, plus a baseline contributing ~4.8%. To definitely assign components of the $P700^+$ dark relaxation to its reaction with F_X^- and to exclude A_1^- as a possible contributor to the observed kinetics, we measured the flash-induced changes in the blue region where the F_X iron-sulfur cluster absorbs (Parrett et al., 1989; Franke et al., 1995).

Both P700 and F_X contribute to absorbance changes in the blue region. Their individual differential spectra can be obtained by using methyl viologen, which functions as an electron acceptor, preventing the back-reaction between F_X^- and $P700^+$ (Yu et al., 1995). In the spectral region from 400 to 480 nm, we found virtually no absorbance changes at 415 nm (Fig. 4) and 445 nm (not shown) in the presence of methyl viologen. Therefore these wavelengths represent the cross-over points of the P700/$P700^+$ difference spectrum. The absorbance change measured at these points in the absence of methyl viologen should be ascribed entirely to a change in the F_X oxidation state. Fig. 4 shows a multiexponential fit of kinetics measured at 415 nm. The major decay phase has a lifetime of 550 μs (61.4%); it is preceded by a 153-μs phase (23.9%) and followed by a 3-ms phase (10.6%) and a slower decaying component approximated with a baseline (4.1%).

The main difference between the measurement of P700-F_X core complexes at 415 nm and 811 nm is the presence of a fast 9-μs component at 811 nm. As we have shown for both P700-F_X core and integral PS I complexes, components with lifetimes of ~10 μs are not saturated with flash energies that saturate the major (hundreds of microseconds to milliseconds) components and hence correspond to the decay of the triplet state of chlorophyll (Vassiliev et al., 1997). It follows that the major kinetic components at 811 nm (576 μs and 3.6 ms) and 415 nm (550 μs and 3 ms) arise from the reaction between F_X^- (directly or via A_1) and $P700^+$. Note that the 250-μs kinetic phase of NIR absorbance change in PS I complexes with F_A and F_B (but not F_X) prereduced by dithionite before the flash was attributed to A_1^- back-reaction and was explained assuming that the $P700^+F_X^-$ state is lower in free energy than the $P700^+A_1$ state when F_A and F_B are prereduced (Brettel, 1989, 1997). This consideration does not apply to the experimental data presented in this paper on PS I complexes devoid of F_A and F_B.

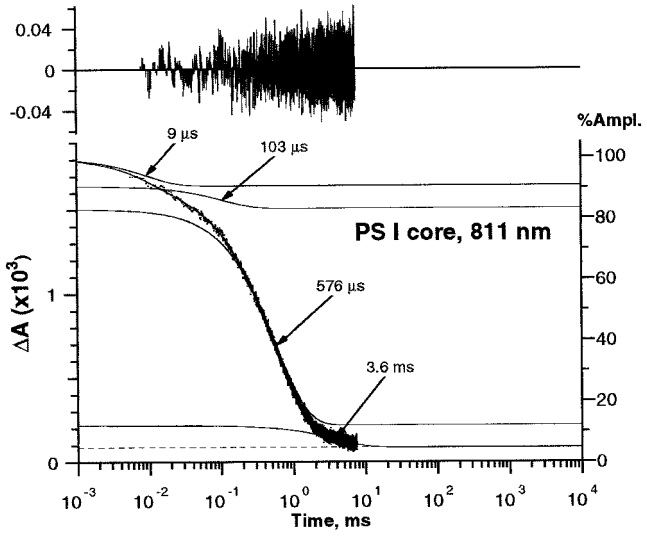

FIGURE 3 Kinetics of absorbance change at 811 nm in P700-F_X core complexes from *Synechococcus* sp. PCC6301. The reaction medium is as in Fig. 1.

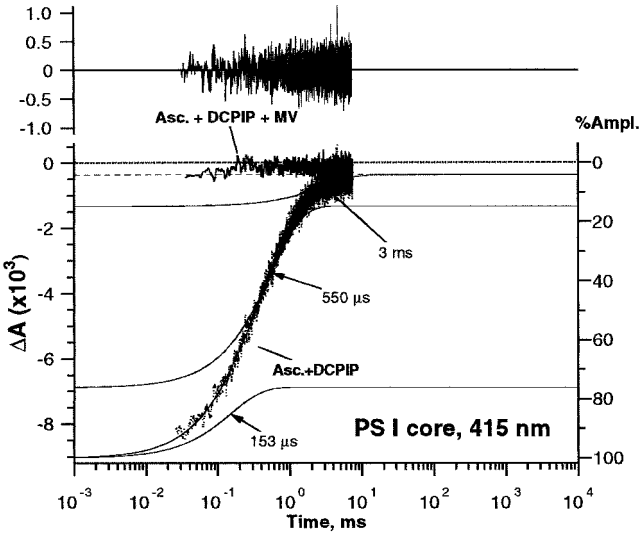

FIGURE 4 Kinetics of absorbance change at 415 nm in P700-F_X core complexes from *Synechococcus* sp. PCC6301 in the absence (*bottom curve*) and in the presence (*curve in the center*) of 280 mM methyl viologen. The reaction medium is as in Fig. 1, but the Chl *a* concentration was 8 μg/ml.

It is generally assumed that the monomolecular back-reaction between a particular acceptor and P700 should follow monoexponential kinetics, but in many instances (see Figs. 1–4) the experimental data are best fitted by two or more components. The nature of this heterogeneity in the dark relaxation of $P700^+$ is not fully understood, but it may be related to the existence of different conformational (sub) states in the reaction clusters. Such a heterogeneity has been reported in PS I (Schlodder et al., 1998) and RCs from purple bacteria (McMahon et al. 1998).

In the following calculations, we use the average time determined as $(\tau_1A_1 + \tau_2A_2 + \tau_3A_3)/(A_1 + A_2 + A_3)$, where τ_i are the lifetimes and A_i are the amplitudes of the single exponentials, corresponding to the same reaction of P^+ dark reduction. Using the multiexponential analysis data from Figs. 3 and 2, we estimate the average lifetimes to be used in further calculations: $\tau_{XP} \approx 0.85$ ms [$= (0.576 \cdot 71.2 + 3.6 \cdot 7.2)/(71.2 + 7.2)$] for the $F_X^- \rightarrow P700^+$ back-reaction in P700-F_X cores and $\tau_{AP} \approx 40.7$ ms [$= (3 \cdot 7.8 + 18 \cdot 44.2 + 112 \cdot 18.2)/(7.8 + 44.2 + 18.2)$] for the $F_A^- \rightarrow P700^+$ back-reaction in $HgCl_2$-treated (F_B-less) PS I complexes.

DISCUSSION

Data from x-ray structural analysis of PS I and low-molecular-mass [4Fe-4S] ferredoxins

The preliminary x-ray structure analysis of crystals of PS I depicts the geometry of iron-sulfur clusters on the acceptor side of PS I (Schubert et al., 1997; Fromme, 1999; Klukas et al., 1999). The center-to-center distance is 15 Å between F_x and F_1 and 12 Å between F_1 and F_2. The x-ray data do not allow one to determine the identity of F_1 and F_2 (see Brettel, 1997, and Kamlowski et al., 1997, for a full discussion). The distance between F_1 and F_2 can be modeled by the bacterial ferredoxins for which precise x-ray structural analysis has been carried out. For example, in the [4Fe-4S] ferredoxin from *Peptococcus asacharolyticus* (formerly *P. aerogenes*; Adman et al., 1976), the closest edge-to-edge distance between the iron atoms in different clusters is 8 Å, while the center-to-center distance is 12 Å, which is in good agreement with the 12-Å distance determined between clusters F_1 and F_2 in PS I.

Application of the relationship between electron transfer rate and distance among the electron carriers on the acceptor side of PS I

The rate of electron transfer between electron carriers decreases exponentially with distance, and this dependence has been tabulated for different reactions in proteins (see, for example, Likhtenshtein, 1988; Moser et al., 1995; Gray and Winkler, 1996). The most detailed "ruler" has been suggested by Dutton and co-workers (Moser et al., 1995), who deduced this relationship from an analysis of electron transfer in photosynthetic proteins. According to this formulation (Moser et al., 1995), the logarithm of the rate constant of intraprotein electron transfer between two electron carriers with edge-to-edge distance R can be described by the following equation:

$$\log k = 15 - 0.6R - 3.1(\Delta G^0 + \lambda)^2/\lambda \qquad (1)$$

where R is the distance in Å, $\Delta G°$ is the standard reaction free energy in eV, and λ is the reorganization energy in eV. The most essential consequence of this dependency is a one-order change in the rate of electron transfer in proteins with a change of distance of 1.7 Å.

Schlodder et al. (1998) estimated from the temperature dependence of electron transport that the reorganization energy for the reaction between A_1 and F_X has a value of ~1 eV. In the following calculations, we assume $\lambda = 1$ eV for reactions between all iron-sulfur clusters in PS I.

By applying Eq. 1 to the acceptor side of PS I, we can estimate (Fig. 5) that the rate of electron transfer between F_X and F_1 and between F_1 and F_2 is faster than 10 μs (see also Brettel, 1997). The distance between F_1 and F_2 and P700 exceeds 35 Å, which requires the experimentally observed millisecond reduction of $P700^+$ by these acceptors to occur indirectly via thermal repopulation of F_X. There-

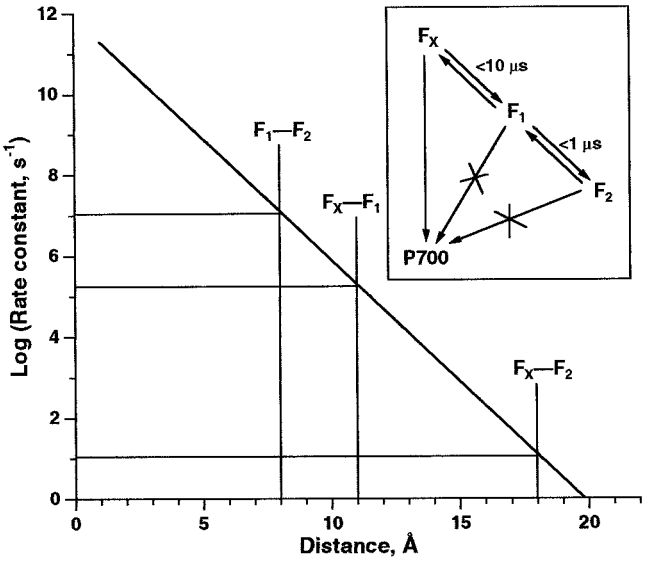

FIGURE 5 Dependence of the logarithm of the rate of electron transfer in biological systems on the distance between cofactors described by Eq. 1 and the suggested rate constants of electron transfer between the acceptors of PS I, based on data of x-ray structural analysis. Values of $\lambda = 1$ eV and $\Delta G^0 = 0$ eV were used in calculations to draw the theoretical line. The edge-to-edge distance between iron sulfur centers (indicated by *vertical lines*) is assumed to be equal to the center-center distance minus 4 Å. *Inset*: Scheme of electron transfer in the PS I derived from application of the correlation between rate of electron transfer and x-ray distances between the cofactors to the data of x-ray structural analysis. The rates of electron transfer from F_1 to P700 and from F_2 to P700 are significantly slower than back-reactions via F_X (directly or via A_1).

fore the distances between the cofactors strongly support a linear chain of electron transfer between F_X, F_1, and F_2 during the dark relaxation of $P700^+$:

$$P700 \leftarrow F_x \leftrightarrow F_1 \leftrightarrow F_2 \tag{2}$$

Fig. 5 (*inset*) shows the scheme of electron transfer in PS I that takes into account these considerations.

Identification of F_1 as F_A, based on an analysis of the kinetics of $P700^+$ dark relaxation in PS I complexes containing only F_A

We now analyze in detail the kinetics of electron transfer between the iron-sulfur clusters of PS I. We make no a priori assumptions about the sequence of electron transfer; rather we consider the two possible positions of F_A and F_B. The linearity of electron transfer between F_X, F_1, and F_2 and the noncontroversial identification of F_X leads to only two alternatives, either $F_A \equiv F_1$ or $F_A \equiv F_2$. Depending on the assumption about the identity of the F_A cluster, the kinetics of the dark relaxation of P700 should be different because of the asymmetrical positions, and hence different distances, of F_1 and F_2 relative to F_X. The results of our theoretical calculations with experimental observations are compared below.

Assumption that $F_1 \equiv F_A$

Let us assume, first, that $F_A \equiv F_1$. In this case the center-to-center distance between F_X and $F_1 \equiv F_A$ is short, ~15 Å, and the edge-to-edge distance can be as short as 11 Å. Applying the rate versus distance dependency to this case (Fig. 5), we find that the rate constant of electron transfer between these clusters is in the range of 10^5–10^6 s^{-1}, i.e., this electron transfer is significantly faster than the back-reaction from F_X^- to $P700^+$ ($\tau \approx 0.85$ ms in P700-F_X core complexes). In this case electron transfer in Hg-treated PS I complexes during dark relaxation can be represented by the following scheme (we ignore the very small minority of PS I complexes with damaged F_A):

$$PF_XF_1 \xleftarrow{k_{XP}} P^+F_X^-F_1 \underset{k_{1X}}{\overset{k_{X1}}{\rightleftarrows}} P^+F_XF_1^- \tag{3}$$

Here P stands for P700. k_{XP}, k_{X1}, and k_{1X} are the respective rate constants of electron transfer. The system of differential equations describing the kinetics of electron transfer according to Scheme 3 is

$$\begin{cases} \dfrac{d[P^+F_X^-F_1]}{dt} = -(k_{XP} + k_{X1})[P^+F_X^-F_1] + k_{1X}[P^+F_XF_1^-] \\ \dfrac{d[P^+F_XF_1^-]}{dt} = k_{X1}[P^+F_X^-F_1] - k_{1X}[P^+F_XF_1^-] \end{cases} \tag{4}$$

Its solution, with the initial conditions $[P^+F_X^-F_1](0) = 1$ and $[P^+F_XF_1^-](0) = 0$, can be written in the following general form:

$$\begin{aligned} [P^+F_X^-F_1] &= \frac{\eta + k_{1X}}{\eta - \mu} e^{\eta t} - \frac{\mu + k_{1X}}{\eta - \mu} e^{\mu t} \\ [P^+F_XF_1^-] &= \frac{k_{X1}}{\eta - \mu} e^{\eta t} - \frac{k_{X1}}{\eta - \mu} e^{\mu t} \end{aligned} \tag{5}$$

where $\eta = -\sigma - \sqrt{\sigma^2 - \rho}$, $\mu = -\sigma + \sqrt{\sigma^2 - \rho}$, and $\sigma = (k_{XP} + k_{1X} + k_{X1})/2$, $\rho = k_{1X}k_{XP}$. When $\sigma^2 \gg \rho$, the η and μ can be approximated by the following simple expressions:

$$\eta \approx -2\sigma; \quad \mu \approx -\rho/2\sigma \tag{6}$$

From Eq. 5 it follows that the normalized kinetics of the dark relaxation of flash-induced P^+ ($\equiv [P^+F_X^-F_1] + [P^+F_XF_1^-]$) according to Scheme 3 is described by two exponential components (*F* stands for the relative amplitude of the fast component, and *S* stands for the relative amplitude of the slow component):

$$[P^+] = \frac{\eta + k_{1X} + k_{X1}}{\eta - \mu} e^{\eta t} - \frac{\mu + k_{1X} + k_{X1}}{\eta - \mu} e^{\mu t} \equiv Fe^{\eta t} + Se^{\mu t} \tag{7}$$

According to Eq. 7 the fraction of the fast component of $P700^+$ dark relaxation is

$$F = (\eta + k_{X1} + k_{1X})/(\eta - \mu) \tag{8}$$

For the case considered here ($F_A \equiv F_1$) the estimated rate constant of electron transfer between F_X and F_1 (10^5-10^6 s^{-1}) is significantly larger than the rate constant of the back-reaction from F_X^- to $P700^+$ (10^3-10^4 s^{-1}), i.e., $k_{X1} \gg k_{XP}$. From Eq. 6 it follows that in this case $\eta \approx -(k_{X1} + k_{1X} + k_{XP})$, $\mu \approx -k_{XP}k_{1X}/(k_{X1} + k_{1X})$. Using these approximations and Eq. 8, we find that the fraction of the fast component is very small:

$$F \approx k_{XP}/(k_{X1} + k_{1X}) \ll 1 \tag{9}$$

Thus the kinetics of $P700^+$ dark relaxation according to Scheme 3 is described by a "slow" exponent with a lifetime,

$$\tau_{sl} \equiv -1/\mu \approx (k_{X1} + k_{1X})/(k_{XP}k_{1X}) \tag{10}$$

This lifetime of $P700^+$ dark relaxation can be derived by assuming equilibrium between iron-sulfur clusters F_X and F_1 during dark relaxation (see, for example, Shinkarev and Wraight, 1993).

From Eq. 10 it follows that the time of the slow millisecond component (2–200 ms) of $P700^+$ dark relaxation, τ_{sl}, is determined by the lifetime of electron transfer from F_X to P700, τ_{XP}, and by the equilibrium constant L_{X1} ($= k_{X1}/k_{1X}$) responsible for redistribution of the electron

between F_X and $F_1 \equiv F_A$:

$$\tau_{sl} = \tau_{XP}(1 + L_{X1}) \quad (11)$$

The fast partitioning of the electron between F_X and F_A in Scheme 3 leads to the absence of any significant F_X component (<2 ms). This agrees well with measured kinetics of $P700^+$ dark relaxation in PS I complexes treated with $HgCl_2$ (Fig. 2), where the slow millisecond F_A/F_B component (2–200 ms) is ~70%.

Assumption that $F_A \equiv F_2$

Let us now assume that $F_A \equiv F_2$. In this case $F_1 = F_B$ is damaged by $HgCl_2$, and the distance between F_X and F_A will be 22 Å (18-Å edge-to-edge distance). According to Fig. 5 this distance corresponds to an optimum rate of electron transfer in the region of 10^1 to 10^2 s^{-1}, i.e., lifetimes of ~10–100 ms. The electron transfer between F_X and $F_A = F_2$ in this case is essentially slower than the back-reaction between F_X^- and $P700^+$, and we can no longer assume a fast equilibrium between F_X and F_2. The scheme of electron transfer in PS I after a single flash will be as follows:

$$PF_XF_2 \xleftarrow{k_{XP}} P^+F_X^-F_2 \underset{k_{2X}}{\overset{k_{X2}}{\rightleftarrows}} P^+F_XF_2^- \quad (12)$$

This scheme is analogous to Scheme 3 considered above. Therefore, the general solution for $P700^+$ dark relaxation (Eqs. 5–8) is valid here, too, if one replaces k_{X1} with k_{X2} and k_{1X} with k_{2X}. However, in the case considered here the rate of electron transfer between F_X and P700 is essentially larger than the rate of electron transfer between F_X and F_A, i.e., $k_{XP} \gg k_{X2}$. In this case $\eta \approx -(k_{XP} + k_{2X} + k_{X2})$, $\mu \approx -k_{2X}$, and the fraction of the fast component is close to 1:

$$F \approx \frac{k_{XP}}{k_{XP} + k_{X2}} \approx 1 \quad (13)$$

Thus, for the case considered here, the fast component will have a time $\approx \tau_{XP}$ and a relative amplitude of $\tau_{X2}/(\tau_{X2} + \tau_{XP}) \approx 1$. Using $\tau_{X2} \approx 10$–100 ms (estimated from Eq. 1 or from Fig. 5) and $\tau_{XP} \approx 0.85$ ms, we can estimate that the fraction of the fast component must be greater than 0.92 and the slow component smaller than 0.08. Thus we see that the assumption that $F_A \equiv F_2$ leads to the conclusion that the amplitude of the slow (~10 and 200 ms) components should be practically zero. This contradicts the experimental data on the kinetics of $P700^+$ dark relaxation in $HgCl_2$-treated PS I complexes presented in Fig. 2. The fraction of the millisecond components (~10 and 200 ms) of $P700^+$ dark relaxation in these preparations is ~70%. This fraction will become even higher after exclusion of the fastest component (12 μs) that arises from either ^{3}Chl formation or from damage to some of the PS I clusters. The presence of a significant fraction of slow component(s) (>70%) coincides well with other results (Fujii et al., 1990; He and Malkin, 1994; Vassiliev et al., 1997; Diaz-Quintana et al., 1998).

Similarly, this scheme predicts that the relative amplitude of the fast component must be greater than 92%. Our experiments (Fig. 2) show that no more than ~8.3% of the submillisecond (0.2–2 ms) phase is present in the kinetics of PS I after treatment with $HgCl_2$. This is significantly less than 92%, which should be observed in this case.

Therefore, we must draw the conclusion that the identity $F_A \equiv F_2$ suggested above is inconsistent with the experimental data. Only the identity $F_A \equiv F_1$ can explain the absence of a significant fast submillisecond (0.2–2 ms) F_X component and the presence of a significant millisecond (2–200 ms) F_A/F_B component, providing a reasonable, noncontradictory description of the dark relaxation of $P700^+$ observed experimentally in $HgCl_2$-treated PS I complexes. Even with the large uncertainties in the theoretical treatment (the value of λ, the geometry of the cubane clusters, and hence the precise edge-to-edge distance), we suggest that the correlation between the rate of electron transfer and distances between cofactors and the theoretical analysis of electron transfer in PS I strongly supports the following sequence of electron transfer: $F_X \rightarrow F_A \rightarrow F_B \rightarrow Fd$. The above considerations are summarized in the flow chart shown in Fig. 6.

From the chart in Fig. 6 one can see that the above conclusion for the sequence of electron transfer on the acceptor side of PS I will be valid insofar as the rate constant of electron transfer between F_X^- and P^+ is larger than the rate constant for the electron transfer between F_X and F_2 and less than the rate constant of electron transfer between F_X and F_1, i.e., $k_{X1} > k_{XP} > k_{X2}$, or

$$\log(k_{X1}) > \log(1/\tau_{XP}) > \log(k_{X2}) \quad (14)$$

Assuming the validity of Eq. 1, we can solve the latter inequality for $(\Delta G^\circ + \lambda)^2/\lambda$:

$$0.36 \le (\Delta G^0 + \lambda)^2/\lambda \le 1.72 \quad (15)$$

Assuming that $\Delta G^\circ = -0.1$ eV, we have the following range for reorganization energies for which this inequality will hold (we used here the relationship $(\Delta G^\circ + \lambda)/\lambda \approx \lambda + 2\Delta G^\circ$, which is valid when $|\lambda| \gg |\Delta G^\circ|$): $0.56 \le \lambda \le 1.92$.

Thus our conclusion about the sequence of electron transport will hold for a wide range of reorganization energies.

Estimation of equilibrium constant of electron transfer between F_X and F_A

The established sequence of electron transfer between the iron-sulfur clusters in PS I allows one to determine the value of the equilibrium constant of electron transfer between F_X

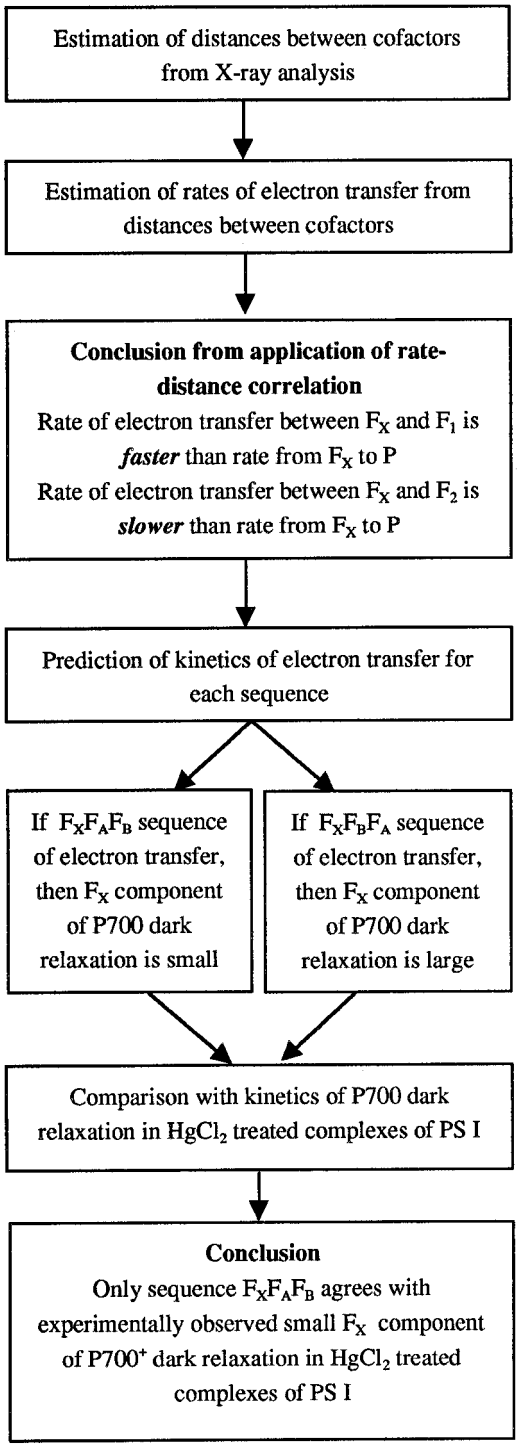

FIGURE 6 The flow chart of the logic for determining the sequence of the electron transfer in the PS I, based on the analysis of the kinetics of $P700^+$ dark relaxation.

and F_A from the kinetics of $P700^+$ dark relaxation. According to Eq. 11 the equilibrium constant of electron transfer between F_X and F_A (L_{XA}) can be estimated from the values of the lifetimes of $P700^+$ dark reduction by F_A^- (τ_{sl}) and by F_X^- (τ_{XP}):

$$L_{XA} = \frac{\tau_{sl} - \tau_{XP}}{\tau_{XP}} \approx \frac{\tau_{sl}}{\tau_{XP}} \tag{16}$$

Based on the kinetics of the P700-F_X core complex (Fig. 3), we estimate that $\tau_{XP} \approx 0.85$ ms. Based on the $P700^+$ reduction kinetics of the $HgCl_2$-treated PS I complex (Fig. 2), we estimate that $\tau_{AP} \approx 41$ ms. Thus $L_{XA} = (41 - 0.85)/0.85 \approx 47$. This value corresponds to a ~100-mV difference between the midpoint potentials of F_X and F_A at room temperature. Note that this calculation uses data from preparations where F_B and where F_A/F_B are missing, thereby avoiding problems with electrostatic interaction from prereduced electron acceptors. A considerably higher value of this equilibrium constant is estimated based on the generally accepted midpoint potentials of the iron-sulfur clusters (F_X, −705 mV (Chamorovsky and Cammack, 1982); F_A, −540 mV (Evans and Heathcote, 1980)), measured using EPR at low temperatures: $L_{XA} = 10^{(705 - 540)/60} \approx 562$.

This discrepancy cannot be resolved by using the lifetime of the main (largest) component of the P^+ reduction by F_X^- instead of the average time used above for the calculation of equilibrium constant L_{XA}. Indeed, according to the data in Fig. 4 this time is equal to 0.55 ms, which corresponds to an equilibrium constant $L_{XA} = (41 - 0.55)/0.55 \approx 73.5$.

One possible reason for the discrepancy is that the midpoint potential of F_X may be affected by electrostatic interaction with F_A^- and F_B^-. This potential was determined by low-temperature EPR under conditions where both F_A and F_B were prereduced (Chamorovsky and Cammack, 1982). A proper comparison with the kinetics of $P700^+$ dark relaxation should use the measurement of midpoint potential of F_X under conditions where both F_A and F_B are oxidized. The influence of an electrostatic interaction between the iron-sulfur clusters on the kinetics and thermodynamics of electron transfer is consistent with the fact that the F_X back-reaction, measured under conditions where both F_A and F_B are reduced by dithionite, is consistently faster than when measured in a P700-F_X core complex. In control and $HgCl_2$-treated TX-PS I complexes in the presence of dithionite at pH 10, where F_A and F_B (when present) are both reduced, the $\tau_{XP} \approx 0.35$ ms and 0.56 ms, respectively (data not shown).

This agrees well with the lower value of the midpoint potential of F_X (−670 mV) estimated for the P700-F_X core complex by transient optical spectroscopy (Parrett et al., 1989). The equilibrium constant estimated using the latter value of the midpoint potential of F_X ($L_{XA} = 10^{(670 - 540)/60} \approx 147$) is closer to the value estimated here from the kinetics of $P700^+$ dark relaxation at room temperature. The other reason for the discrepancy may be a possible temperature dependence of the equilibrium constant of electron transfer between F_X and F_A.

Rationale for uphill electron transfer on the acceptor side of PS I

The values of midpoint redox potentials of iron-sulfur clusters in PS I (-540 mV for F_A and -590 mV for F_B) indicate the presence of an uphill electron transfer between F_A and F_B. This needs to be examined from a functional point of view. Such an uphill electron transfer step assumes that the redox equilibrium between F_A and F_B will be shifted toward F_A. Low-potential exogenous acceptors of electrons in PS I can interact with oxygen and produce superoxide O_2^-. The interaction of F_A with oxygen is slower than with F_B (at least in the presence of MV) (Fujii et al., 1990; Vassiliev et al., 1998). Thus redistribution of the electron to the F_A cluster will decrease the rate of electron donation from F_B to oxygen when ferredoxin is not in its binding site and should thereby maintain a high quantum yield of $NADP^+$ reduction relative to formation of O_2^-. It may also protect the reaction center from oxidative destruction by O_2^-. At the same time, the total driving force for electron transfer to ferredoxin bound to the F_B site is energetically favorable and will be sufficient for nearly irreversible transfer of the electron to ferredoxin.

Using an equation similar to Eq. 16, we can estimate the equilibrium constant of electron transfer between F_A and F_B at room temperature as $0.8 \leq L_{AB} \leq 4.5$. The range of values of the equilibrium constant is determined by the range of average lifetimes of the main components of $P700^+$ dark relaxation. This estimate shows that the energy difference between F_A and F_B at room temperature is less than that predicted by the values of the redox potentials. This is likely because the redox potential of F_B was experimentally determined by EPR in the presence of reduced F_A. The redox potentials of F_A and F_B were also determined under conditions where ferredoxin (or flavodoxin) is not bound to the PS I complexes. Binding of ferredoxin (or flavodoxin) may change the equilibrium constant of electron transfer between F_A and F_B. We will report elsewhere a study of the thermodynamics of electron transport between F_A and F_B at room temperature in an attempt to further explore the issue of uphill electron transfer on the acceptor side of PS I.

CONCLUSIONS

We show that the kinetics of $P700^+$ dark relaxation in the presence of F_A only and in the presence of both F_A and F_B can be used to identify the sequence of electron transfer through the iron-sulfur clusters F_A and F_B. By applying the dependence of the electron transfer rate versus distance to the kinetics of electron transfer in PS I, and by taking into consideration the asymmetrical position of iron-sulfur clusters F_A and F_B relative to F_X, we are able to determine that the sequence of electron transfer is $F_X \rightarrow F_A \rightarrow F_B$ ($\rightarrow$ Fd). Using this sequence of electron transfer during $P700^+$ dark relaxation, we estimate that the equilibrium constant between F_X and F_A at room temperature is ~ 47 in $HgCl_2$-treated (F_B-less) PS I complexes.

Note added in proof: On the basis of a comparison between experimental and theoretical values of spin relaxation enhancement effects on $P700^+$ in PS I particles containing and lacking the F_B cluster, Lakshmi, Jung, Golbeck, and Brudvig recently showed that iron-sulfur cluster F_A is closer to P700 than the F_B cluster. This agrees with the orientation for F_A and F_B determined in the present study. Biochemistry 1999, 38: 13210–13215.

This work was supported by a grant to JHG from the National Science Foundation (MCB-9723661).

REFERENCES

Adman, E. T., L. C. Sieker, and L. H. Jensen. 1976. Structure of *Peptococcus aerogenes* ferredoxin. I. Refinement at 2 Å resolution. *J. Biol. Chem.* 251:3801–3806.

Brettel, K. 1989. New assignment for the 250 μs kinetics of photosystem I: $P\text{-}700^+$ recombines with A_1^- (not F_X^-). *Biochim. Biophys. Acta.* 976:246–249.

Brettel, K. 1997. Electron transfer and arrangement of the redox cofactors in photosystem I. *Biochim. Biophys. Acta.* 1318:322–373.

Brettel, K., and J. H. Golbeck. 1995. Spectral and kinetic characterization of electron acceptor A_1 in a photosystem I core devoid of iron-sulfur centers F_X, F_B and F_A. *Photosynth. Res.* 45:183–193.

Chamorovsky, S. K., and R. Cammack. 1982. Direct determination of the midpoint potential of the acceptor X in chloroplast photosystem I by electrochemical reduction and ESR spectroscopy. *Photobiochem. Photobiophys.* 4:195–200.

Diaz-Quintana, A., W. Leibl, H. Bottin, and P. Sétif. 1998. Electron transfer in photosystem I reaction centers follows a linear pathway in which iron-sulfur cluster F_B is the immediate electron donor to soluble ferredoxin. *Biochemistry.* 37:3429–3439.

Evans, M. C. W., and P. Heathcote. 1980. Effects of glycerol on the redox properties of the electron acceptor complex in spinach photosystem I particles. *Biochim. Biophys. Acta.* 590:89–96.

Fischer, N., P. Sétif, and J. D. Rochaix. 1997. Targeted mutations in the psaC gene of *Chlamydomonas reinhardtii*: preferential reduction of F_B at low temperature is not accompanied by altered electron flow from photosystem I ferredoxin. *Biochemistry.* 36:93–102.

Fischer, N., P. Sétif, and J. D. Rochaix. 1999. Site-directed mutagenesis of the PsaC subunit of photosystem I—F_B is the cluster interacting with soluble ferredoxin. *J. Biol. Chem.* 274:23333–23340.

Franke, J. F., L. Ciesla, and J. T. Warden. 1995. Kinetics of PsaC reduction in photosystem I. *In* Photosynthesis: From Light to Biosphere, Vol. 2. P. Mathis, editor. Kluwer Academic Publishers, Dordrecht, the Netherlands. 75–78.

Fromme, P. 1999. Biology of photosystem I: structural aspects. *In* Concepts in Photobiology: Photosynthesis and Photomorphogenesis. G. S. Singhal, G. Renger, S. K. Sopory, K. D. Irrgang, and Govindjee, editors. Narosa Publishing House, New Delhi. 181–220.

Fujii, T., E. I. Yokoyama, K. Inoue, and H. Sakurai. 1990. The sites of electron donation of photosystem I to methyl viologen. *Biochim. Biophys. Acta.* 1015:41–48.

Golbeck, J. H. 1995. Resolution and reconstitution of photosystem I. *In* CRC Handbook of Organic Photochemistry and Photobiology. P. S. Song and W. M. Horspool, editors. CRC Press, Boca Raton, FL. 1407–1419.

Golbeck, J. H. 1999. A comparative analysis of the spin state distribution of in vitro and in vivo mutants of PsaC. A biochemical argument for the sequence of electron transfer as $F_X \rightarrow F_A \rightarrow F_B \rightarrow$ ferredoxin. *Photosynth. Res.* 61:107–144.

Golbeck, J. H., and J. Warden. 1982. Electron spin resonance studies of the bound iron-sulfur centers in photosystem I. Photoreduction of center A occurs in the absence of center B. *Biochim. Biophys. Acta.* 681:77–84.

Gray, H. B., and J. R. Winkler. 1996. Electron transfer in proteins. *Annu. Rev. Biochem.* 65:537–561.

Hanley, J., J. Kear, G. Bredenkamp, G. Li, P. Heathcote, and M. C. W. Evans. 1992. Biochemical evidence for the role of the bound iron-sulphur centre-B in NADP reduction by photosystem I. *Biochim. Biophys. Acta.* 1099:152–156.

He, W. Z., and R. Malkin. 1994. Reconstitution of iron-sulfur center B of photosystem I damaged by mercuric chloride. *Photosynth. Res.* 41: 381–388.

Jung, Y. S., L. Yu, and J. H. Golbeck. 1995. Reconstitution of iron-sufur center F_A results in complete restoration of NADP(+) photoreduction in Hg-treated Photosystem I complexes from *Synechococcus* sp. PCC 6301. *Photosynth. Res.* 46:249–255.

Kamlowski, A., A. Van der Est, P. Fromme, N. Krauss, W. D. Schubert, O. Klukas, and D. Stehlik. 1997. The structural organization of the psaC protein in photosystem I from single crystal EPR and x-ray crystallographic studies. *Biochim. Biophys. Acta.* 1319:199–213.

Klukas, O., W. D. Schubert, P. Jordan, N. Krauss, P. Fromme, H. T. Witt, and W. Saenger. 1999. Photosystem I, an improved model of the stromal subunits PsaC, PsaD, and PsaE. *J. Biol. Chem.* 274:7351–7360.

Likhtenshtein, G. I. 1988. Chemical Physics of Redox Metalloenzyme Catalysis. Springer-Verlag, Berlin.

Malkin, R. 1984. Diazonium modification of photosystem I. A specific effect on iron-sulfur center B. *Biochim. Biophys. Acta.* 764:63–69.

Mamedov, M. D., K. N. Gourovskaya, I. R. Vassiliev, J. H. Golbeck, and A. Y. Semenov. 1998. Electrogenicity accompanies photoreduction of the iron-sulfur clusters F_A and F_B in photosystem I. *FEBS Lett.* 431: 219–223.

Manna, P., and P. R. Chitnis. 1999. Function and molecular genetics of photosystem I. *In* Concepts in Photobiology: Photosynthesis and Photomorphogenesis. G. S. Singhal, G. Renger, S. K. Sopory, K. D. Irrgang, and Govindjee, editors. Narosa Publishing House, New Delhi. 221–263.

McMahon, B. H., J. D. Müller, C. A. Wraight, and G. U. Nienhaus. 1998. Electron transfer and protein dynamics in the photosynthetic reaction center. *Biophys. J.* 74:2567–2587.

Moser, C. C., C. C. Page, R. Farid, and P. L. Dutton. 1995. Biological electron transfer. *J. Bioenerg. Biomembr.* 27:263–274.

Naver, H., M. P. Scott, J. H. Golbeck, B. L. Møller, and H. V. Scheller. 1996. Reconstitution of barley photosystem I with modified PSI-C allows identification of domains interacting with PSI-D and PSI-A/B. *J. Biol. Chem.* 271:8996–9001.

Parrett, K., T. Mehari, P. G. Warren, and J. H. Golbeck. 1989. Purification and properties of the intact P700 and Fx-containing photosystem I core protein. *Biochim. Biophys. Acta.* 973:324–332.

Sakurai, H., K. Inoue, T. Fujii, and P. Mathis. 1991. Effects of selective destruction of iron-sulfur center B on electron transfer and charge recombination in Photosystem I. *Photosynth. Res.* 27:65–21.

Sauer, K., P. Mathis, S. Acker, and J. A. Van Best. Electron acceptors associated with P-700 in Triton solubilized Photosystem I particles from spinach chloroplasts. *Biochim. Biophys. Acta.* 503:120–134.

Scheller, H. V., H. Naver, and B. L. Møller. 1997. Molecular aspects of photosystem I. *Physiol. Plant.* 100:842–851.

Schlodder, E., K. Falkenberg, M. Gergeleit, and K. Brettel. 1998. Temperature dependence of forward and reverse electron transfer from A_1^-, the reduced secondary electron acceptor in photosystem I. *Biochemistry.* 37:9466–9476.

Schubert, W. D., O. Klukas, N. Krauss, W. Saenger, P. Fromme, and H. T. Witt. 1997. Photosystem I of *Synechococcus elongatus* at 4 Å resolution: comprehensive structure analysis. *J. Mol. Biol.* 272:741–769.

Shinkarev, V. P., and C. A. Wraight. 1993. Electron and proton transfer in the acceptor quinone complex of reaction centers of phototrophic bacteria. *In* The Photosynthetic Reaction Center, Vol. 1. J. Deisenhofer and J. Norris, editors. Academic Press, New York. 193–255.

Vassiliev, I. R., Y. S. Jung, M. D. Mamedov, A. Yu. Semenov, and J. H. Golbeck. 1997. Near-IR absorbance changes and electrogenic reactions in the microsecond-to-second time domain in photosystem I. *Biophys. J.* 72:301–315.

Vassiliev, I. R., Y. S. Jung, F. Yang, and J. H. Golbeck. 1998. PsaC subunit of photosystem I is oriented with iron-sulfur cluster F_B as the immediate electron donor to ferredoxin and flavodoxin. *Biophys. J.* 74:2029–2035.

Yu, J., L. B. Smart, Y. S. Jung, J. H. Golbeck, and L. McIntosh. 1995. Absence of PsaC allows assembly of photosystem I core but prevents binding of PsaD and PsaE in *Synechocystis* sp. PCC 6803. *Plant Mol. Biol.* 29:331–342.